

Enhanced diffraction by a rectangular grating made of a negative phase-velocity (or negative index) material

*Ricardo A. Depine*¹

Departamento de Física, Facultad de Ciencias Exactas y Naturales,
Universidad de Buenos Aires, 1428 Buenos Aires, Argentina

*Akhlesh Lakhtakia*²

Department of Engineering Science and Mechanics, Pennsylvania State University,
University Park, PA 16802-6812, USA

*David R. Smith*³

Department of Electrical and Computer Engineering, Duke University,
Durham, NC 27708, USA

Abstract. The diffraction of electromagnetic plane waves by a rectangular grating formed by discrete steps in the interface of a homogeneous, isotropic, linear, negative phase-velocity (negative index) material with free space is studied using the semi-analytic C method. When a nonspecular diffracted order is of the propagating type, coupling to that order is significantly larger for a negative index material than for conventional material. The computed coupling strengths reported here are in agreement with recent experiments, and illustrate the role of evanescent fields localized at the grating interface in producing this enhanced coupling.

PACS: 42.25.Fx, 78.20.Ci

Keywords: diffraction, grating, negative phase velocity, negative refractive index

¹Corresponding Author. E-mail: rdep@df.uba.ar

²E-mail: akhlesh@psu.edu

³E-mail: drsmith@ee.duke.edu

The study of electromagnetic fields received a major boost in 2001 with the experimental confirmation of negative refraction by dielectric–magnetic materials with negative real permittivity and negative real permeability [1]. When considered as linear, isotropic and homogeneous, these materials possess a complex–valued refractive index whose real part is negative, and are therefore often called *negative index* (NI) materials. Alternatively, these materials can be referred to as *negative phase–velocity* (NPV) materials, as the phase velocity and the time–averaged Poynting vectors therein are antiparallel. Other names are also in circulation; but, regardless of the name used, the common observable phenomenon is negative refraction [2, 3, 4].

All experimental realizations of NPV materials thus far are as periodically patterned composite materials. The unit cell comprises various arrangements of conducting filaments in order to realize both dielectric and magnetic response properties in the same frequency range. For such a material to be considered as effectively homogeneous, the unit cell must be electrically small — i.e., it must be considerably smaller than the free–space wavelength as well as the wavelength in the material [5]. In the wedge sample used by Shelby *et al.* [1], the unit cell size was about one–sixth of the free–space wavelength. The finite size of the unit cell meant that one of the two exposed surfaces of the sample was not planar, but rather formed a rectangular grating [6]. Because of this grating, the specular (or zeroth–order) reflected/refracted plane wave *could* be accompanied by nonspecular (higher–order) diffracted plane waves [6].

Recently, using Ansoft’s HFSS package, an electromagnetics equation solver based on the finite–element method, Smith *et al.* [7] examined the plane–wave response of a wedge having the same properties as that used by Shelby *et al.* [1]. One of the two exposed surfaces was set up as a shallow rectangular grating. The simulation revealed not only a zeroth–order transmitted plane wave but also, unexpectedly, a strong first–order transmitted plane wave. The latter was much stronger for a NPV wedge than for a wedge with identical dimensions but made of a positive phase–velocity (PPV) material. Although

higher-order refracted plane waves were not experimentally observed by Shelby *et al.* [1], the first-order was definitively present in later experiments [4, 7].

While full-wave simulations confirm the phenomenon of enhanced diffraction at the NPV grating, the numerical results are not of use in determining the physical origin of the effect. An alternative approach is furnished by mathematical treatments of diffraction by gratings based on analytic field expansions. These treatments have continued to develop over the last hundred years, and have now acquired a considerable degree of sophistication. We apply one of these methods here, the so-called C method, both to independently verify the simulation results obtained by the finite-element method and to provide further insight as to the underlying mechanism [7]. The C method, originally developed for dielectric gratings [8], was modified to handle dielectric-magnetic gratings [9].

In a rectangular coordinate system (x, y, z) , we consider the periodically corrugated boundary $y = g(x) = g(x + d)$ between vacuum and a homogeneous, isotropic, dielectric-magnetic material, with d being the corrugation period, as shown in Figure 1. The region $y > g(x)$ is vacuum, whereas the medium occupying the region $y < g(x)$ is characterized by complex-valued scalars $\epsilon_2 = \epsilon_{2R} + i\epsilon_{2I}$ and $\mu_2 = \mu_{2R} + i\mu_{2I}$, such that $\epsilon_{2I} \geq 0$ and $\mu_{2I} \geq 0$. The refracting medium is assumed to be *effectively* homogeneous at the angular frequency of interest. A linearly polarized electromagnetic plane wave is incident on this boundary from the region $y > g(x)$ at an angle θ_0 , ($|\theta_0| < \pi/2$), with respect to the y axis.

Let the function $f(x, y)$ represent the z -directed component of the total electric field for the s -polarization case, and the z -directed component of the total magnetic field for the p -polarization case [10]. Outside the corrugations, $f(x, y)$ is rigorously represented by

Rayleigh expansions [11] as

$$f(x, y) = \exp \left[i (\alpha_0 x - \beta_0^{(1)} y) \right] + \sum_{n=-\infty}^{+\infty} \rho_n \exp \left[i (\alpha_n x + \beta_n^{(1)} y) \right], \quad y > \max g(x), \quad (1)$$

and

$$f(x, y) = \sum_{n=-\infty}^{+\infty} \tau_n \exp \left[i (\alpha_n x - \beta_n^{(2)} y) \right], \quad y < \min g(x). \quad (2)$$

Here, $\{\rho_n\}_{n=-\infty}^{+\infty}$ and $\{\tau_n\}_{n=-\infty}^{+\infty}$ are scalar coefficients to be determined; and

$$\left. \begin{aligned} \alpha_0 &= \frac{\omega}{c} \sin \theta_0, \quad \alpha_n = \alpha_0 + 2n\pi/d \\ \beta_n^{(1)} &= \sqrt{\frac{\omega^2}{c^2} - \alpha_n^2}, \quad \beta_n^{(2)} = \sqrt{\frac{\omega^2}{c^2} \epsilon_2 \mu_2 - \alpha_n^2} \end{aligned} \right\}, \quad (3)$$

where c is the speed of light in vacuum and ω is the angular frequency. Note that $\beta_n^{(1)}$ is either purely real or purely imaginary; and the conditions $\text{Re} [\beta_n^{(1)}] \geq 0$ and $\text{Im} [\beta_n^{(1)}] \geq 0 \forall n$ are appropriate for plane waves in the vacuous half-space $y > \max g(x)$. The refracted plane waves must attenuate as $y \rightarrow -\infty$, imposing the condition $\text{Im} [\beta_n^{(2)}] > 0$. Fulfillment of this condition automatically fixes the sign of $\text{Re} [\beta_n^{(2)}]$, regardless of the signs of ϵ_{2R} and μ_{2R} .

After implementing the C method on a computer, the coefficients $\{\rho_n\}_{n=-\infty}^{+\infty}$ and $\{\tau_n\}_{n=-\infty}^{+\infty}$ are determined. Diffraction efficiencies $e_n^\rho = (\text{Re} [\beta_n^{(1)}] / \beta_0^{(1)}) |\rho_n|^2$ are defined for the reflected orders. If dissipation in the refracting medium is small enough to be ignored, diffraction efficiencies $e_n^\tau = (\text{Re} [\beta_n^{(2)}] / \sigma \beta_0^{(1)}) |\tau_n|^2$ are defined for the refracted orders, where either $\sigma = \mu_2$ (s -polarization) or $\sigma = \epsilon_2$ (p -polarization).

The grating of Shelby *et al.* [1] has a rectangular profile, shown in Figure 1, with the long and the short sides in the ratio 3 : 1 and period $d = 15.81$ mm. To simulate this profile for

the C method, $g(x)$ was replaced by the truncated Fourier sum $\sum_{n=0}^{10} \gamma_n \sin(2\pi nx/d + \varphi_n)$, which was found adequate to represent the grating profile.

In Figure 2, we show the diffraction efficiencies obtained as functions of θ_0 at a frequency of 11.75 GHz, the highest frequency used by Smith *et al.* [7], which corresponds to $\omega d/c = 2\pi/1.58$. The refracting medium is of either the NPV ($\epsilon_2 = -5 + i0.01$, $\mu_2 = -1 + i0.01$) or the PPV ($\epsilon_2 = 5 + i0.01$, $\mu_2 = 1 + i0.01$) type. Calculations were made for both the s - and the p -polarization incidence conditions. As confirmed by perturbation analysis [12], in this case the transformation $\{\epsilon \rightarrow -\epsilon^*, \mu \rightarrow -\mu^*\}$ does not greatly affect e_0^ρ (Fig. 2a), except at low $|\theta_0|$. In contrast, Figs. 2b and 2c show that the nonspecular reflection efficiencies $e_{\pm 1}^\rho$, are significantly affected by the type of the refracting medium. In particular, the interplay between the polarization state and the angle of incidence leads to (i) very little difference for the PPV grating between the two polarizations; (ii) considerable difference for the NPV grating between the two polarizations, and (iii) a shift of the difference between PPV and NPV gratings from one polarization to the other as the sign of the angle of incidence changes. As the refracting medium is dissipative, diffraction efficiencies for the refracted orders cannot be defined.

To study refraction efficiencies explicitly, we made the refracting material nondissipative ($\epsilon_2 = \pm 5$, $\mu_2 = \pm 1$), while the other parameters were kept the same. The higher-order reflection efficiency curves display the same qualitative behaviors as in Figure 2, and are therefore not shown in Figure 3. All refraction efficiencies are greatly affected by the type of the refracting medium, as becomes clear from Figs. 3a–c. In particular, the coupling of power into the $n = \pm 1$ refracted orders (Figs. 3b and c) for the NPV grating is much larger than for a PPV grating, a fact that again is in agreement with the results of Smith *et al.* [7].

A similar conclusion is drawn from Figure 4, for which the efficiency curves were computed at a frequency of 9.0 GHz (the smallest frequency used by Smith *et al.* [7]), the

other parameters being the same as in Figure 3. Whereas the zeroth-order (Fig. 4a, the only propagating order reflected at this frequency) reflection efficiency is much less affected by the type of the refracting medium than in our previous examples, the refraction efficiencies depend strongly on the refracting medium being of the PPV or the NPV type.

The increased coupling into higher-order diffracted plane waves represents an important distinction between the behaviors of PPV and NPV materials, and confirms that surface periodicity plays a much more significant role in the latter [7]. The physical origin of the enhanced higher-order reflection efficiencies for the NPV grating can be understood in an approximate manner by examining the reflection efficiencies for shallow gratings. In general, a grating couples the specular coefficients (ρ_0 and τ_0) with all nonspecular coefficients (ρ_n and τ_n , $|n| > 0$) [6], thereby coupling e_0^ρ with all e_n^ρ , $|n| > 0$. All coefficients for a grating of arbitrary profile are obtained together by some numerical technique.

In the limit of the grating profile becoming planar, the reflection coefficients (and, therefore, the efficiencies) coincide with those for a planar interface. The introduction of shallow corrugations only slightly perturbs the coefficients [13], and we may then write

$$\rho_n \simeq -\frac{\beta_n^{(2)} - \sigma\beta_n^{(1)}}{\beta_n^{(2)} + \sigma\beta_n^{(1)}}. \quad (4)$$

In the limit of small dissipation, $\beta_n^{(2)}$ is real-valued for propagating orders in the refracting medium. As this medium transforms from PPV to NPV, $\beta_n^{(2)}$ changes sign along with σ , and the magnitude of ρ_n is thus unchanged. But for evanescent (nonspecular) orders, $\beta_n^{(2)}$ is imaginary, and thus always positive in accordance with causality. Hence, for nonspecular orders, the reflection coefficients are inverted as the refracting medium is transformed from PPV to NPV. The evanescent orders then, which play a minor role for the PPV grating, mediate a much larger interaction between the specular and the nonspecular modes for the NPV grating.

Equation (4) shows that there is the possibility of a pole for one or more reflection orders. A pole indicates the presence of a bound surface mode, identical to the surface

plasmon that occurs at the interface with a metal at optical wavelengths. At least in a perturbative sense, the enhanced diffraction by a NPV grating has the same origin as other plasmon-mediated effects, including enhanced light transmission [14] and the “perfect lens” effect [15].

The detailed treatment presented here of diffraction from a NPV grating reveals enhanced diffraction, in agreement with recent experiments. As NPV materials are considered for various applications, the results found here indicate that great care is necessary in describing the surfaces of NPV materials. In particular, the recent artificially structured metamaterials are based on periodic cells, whose inherent periodicity can lead to a quite significant surface nonhomogeneity, which may assume even greater importance for surfaces that are not nominally planar.

Acknowledgments. R.A.D. acknowledges partial support from CONICET (Grant: ANPCYT-BID 802/OC-AR03-04457), and A.L. from the Mercedes Foundation.

References

- [1] R.A. Shelby, D.R. Smith, S. Schultz, *Science* 292 (2001) 77.
- [2] A. Grbic, G.V. Eleftheriadis, *J. Appl. Phys.* 92 5930 (2002).
- [3] C.G. Parazzoli, R.B. Greegor, K. Li, B.E.C. Koltenbah, M. Tanielian, *Phys. Rev. Lett.* 90 (2003) 107401.
- [4] A. Houck, J. Brock, I. Chuang, *Phys. Rev. Lett.* 90 (2003) 137401.
- [5] H.C. van de Hulst, *Light Scattering by Small Particles* (Dover Press, New York, NY, USA, 1981).

- [6] D. Maystre (ed), *Selected Papers on Diffraction Gratings*, (SPIE Press, Bellingham, WA, USA, 1993).
- [7] D.R. Smith, P.M. Rye, J.J. Mock, D.C. Vier, A.F. Starr, Phys. Rev. Lett. 93 (2004) 137405.
- [8] L. Li, J. Chandezon, J. Opt. Soc. Am. A 13 (1996) 2247.
- [9] R.A. Depine and A. Lakhtakia, arXiv:physics/0408050.
- [10] M. Born, E. Wolf, *Principles of Optics, 6th ed* (Pergamon Press, Oxford, United Kingdom, 1980).
- [11] Lord Rayleigh, Proc. R. Soc. Lond. A 79 (1907) 399.
- [12] R.A. Depine, A. Lakhtakia, Opt. Commun. 233 (2004) 277.
- [13] T. Tamir, S.T. Peng, Appl. Phys. 14 (1977) 235.
- [14] T.W. Ebbesen, H.J. Lezec, H.F. Ghaemi, T. Thio, P.A. Wolff, Nature 391 (1998) 667.
- [15] J.B. Pendry, D.R. Smith, Phys. Today 57 (2004) 37 (June issue).

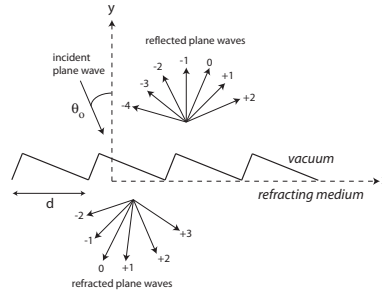


Figure 1: Schematic of the diffraction problem solved. The refracted plane waves are shown as if the refracting medium is of the NPV type. The specular reflected and refracted orders are denoted by $n = 0$, while nonspecular orders are denoted by $n \neq 0$. The inset shows the shape of the grating profile used by Smith *et al.* [7] as well as for Figures 2–4.

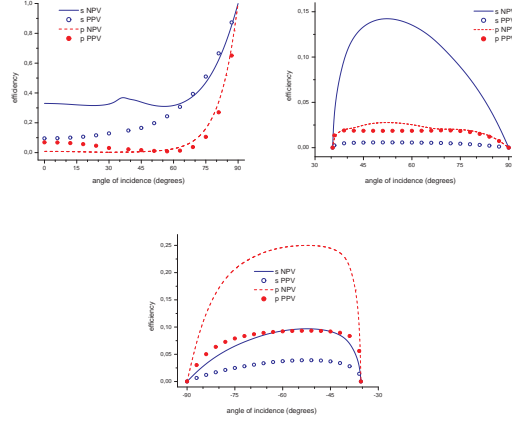


Figure 2: Computed diffraction efficiencies as functions of the angle of incidence θ_0 , when $\omega d/c = 2\pi/1.58$, for both p - and s -polarized plane waves. The refracting medium is either of the PPV ($\epsilon_2 = 5 + i0.01$, $\mu_2 = 1 + i0.01$) or the NPV ($\epsilon_2 = -5 + i0.01$, $\mu_2 = -1 + i0.01$) type. (a) e_0^ρ ; (b) e_{-1}^ρ ; (c) e_{+1}^ρ .

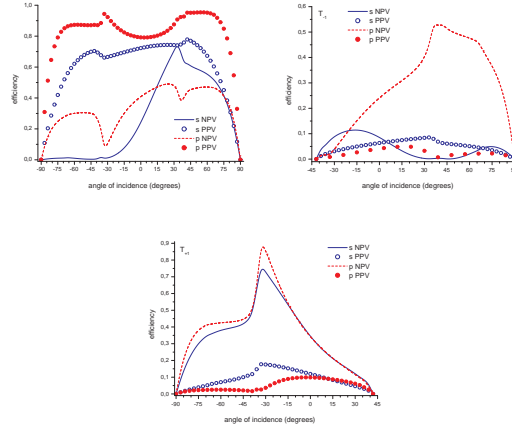


Figure 3: Computed diffraction efficiencies as functions of the angle of incidence θ_0 , when $\omega d/c = 2\pi/1.58$, for both p - and s -polarized plane waves. The refracting medium is either of the PPV ($\epsilon_2 = 5$, $\mu_2 = 1$) or the NPV ($\epsilon_2 = -5$, $\mu_2 = -1$) type. (a) e_0^τ ; (b) e_{-1}^τ ; (c) e_{+1}^τ .

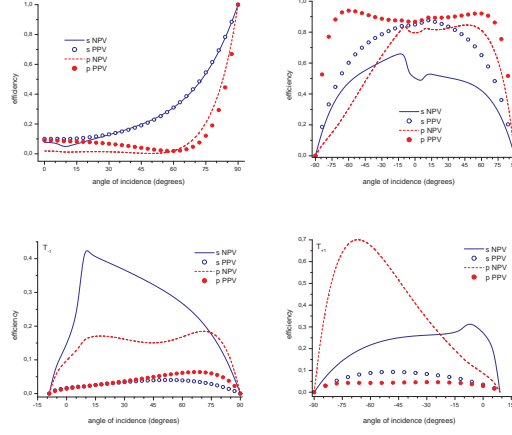


Figure 4: Computed diffraction efficiencies as functions of the angle of incidence θ_0 , when $\omega d/c = 2\pi/2.087$, for both p - and s -polarized plane waves. The refracting medium is either of the PPV ($\epsilon_2 = 5$, $\mu_2 = 1$) or the NPV ($\epsilon_2 = -5$, $\mu_2 = -1$) type. (a) e_0^ρ ; (b) e_0^τ ; (c) e_{-1}^τ ; (d) e_{+1}^τ .